J Biomol NMR (2012) 54:155–168
DOI 10.1007/s10858-012-9659-9

ARTICLE

Optimal degree of protonation for ^{1}H detection of aliphatic sites in randomly deuterated proteins as a function of the MAS frequency

Sam Asami · Kathrin Szekely · Paul Schanda · Beat H. Meier · Bernd Reif

Received: 8 February 2012 / Accepted: 8 August 2012 / Published online: 23 August 2012

Abstract The ^{1}H dipolar network, which is the major obstacle for applying proton detection in the solid-state, can be reduced by deuteration, employing the RAP (Reduced Adjoining Protonation) labeling scheme, which yields random protonation at non-exchangeable sites. We present here a systematic study on the optimal degree of random sidechain protonation in RAP samples as a function of the MAS (magic angle spinning) frequency. In particular, we compare ^{1}H sensitivity and linewidth of a microcrystalline protein, the SH3 domain of chicken α-spectrin, for samples, prepared with 5–25 % H_2O in the *E. coli* growth medium, in the MAS frequency range of 20–60 kHz. At an external field of 19.96 T (850 MHz), we find that using a proton concentration between 15 and 25 % in the M9 medium yields the best compromise in terms of sensitivity and resolution, with an achievable average ^{1}H linewidth on the order of 40–50 Hz. Comparing sensitivities at a MAS frequency of 60 versus 20 kHz, a gain in sensitivity by a factor of 4–4.5 is observed in INEPT-based ^{1}H detected 1D ^{1}H,^{13}C correlation experiments. In total, we find that spectra recorded with a 1.3 mm rotor at 60 kHz have almost the same sensitivity as spectra recorded with a fully packed 3.2 mm rotor at 20 kHz, even though ~20× less material is employed. The improved sensitivity is attributed to ^{1}H line narrowing due to fast MAS and to the increased efficiency of the 1.3 mm coil.

Keywords Magic angle spinning (MAS) solid-state NMR · Perdeuteration · ^{2}H-labeling · Aliphatic resonances · Linewidth · Sensitivity · 1.3 mm rotors · Reduced Adjoining Protonation (RAP)

S. Asami · B. Reif
Helmholtz-Zentrum München (HMGU), Deutsches Forschungszentrum für Gesundheit und Umwelt (HMGU), Ingolstädter Landstr. 1, 85764 Neuherberg, Germany

S. Asami · B. Reif
Leibniz-Institut für Molekulare Pharmakologie (FMP), Robert-Rössle-Straße 10, 13125 Berlin, Germany

K. Szekely · P. Schanda · B. H. Meier
Eidgenössische Technische Hochschule Zürich (ETH Zürich), Wolfgang-Pauli-Str. 10, 8093 Zürich, Switzerland

P. Schanda
Institut de Biologie Structurale Jean-Pierre Ebel, CEA-CNRS-UJF, 41, rue Jules Horowitz, 38027 Grenoble, France

B. Reif (✉)
Department of Chemistry, Munich Center for Integrated Protein Science at Department Chemie (CIPS-M), Technische Universität München (TUM), Lichtenbergstr. 4, 85747 Garching, Germany
e-mail: reif@tum.de

Introduction

Solid-state nuclear magnetic resonance spectroscopy has evolved to an important tool in structural biology, allowing nowadays structural investigations of crystalline and non-crystalline systems (Castellani et al. 2002; Ferguson et al. 2006; Franks et al. 2008; Wasmer et al. 2008). As for any spectroscopic technique, resolution and sensitivity are the main limitations. In terms of sensitivity, protons should be best suited for detection due to their high gyromagnetic ratio. However, due to strong ^{1}H, ^{1}H dipolar couplings, proton resonances are poorly resolved in uniformly protonated samples. In the last two decades, homonuclear decoupling sequences were introduced (Bielecki et al. 1989; Levitt et al. 1993; Vinogradov et al. 1999; Sakellariou et al. 2000; Bosman et al. 2004), reducing proton linewidths to 100–500 Hz. Uniform deuteration of

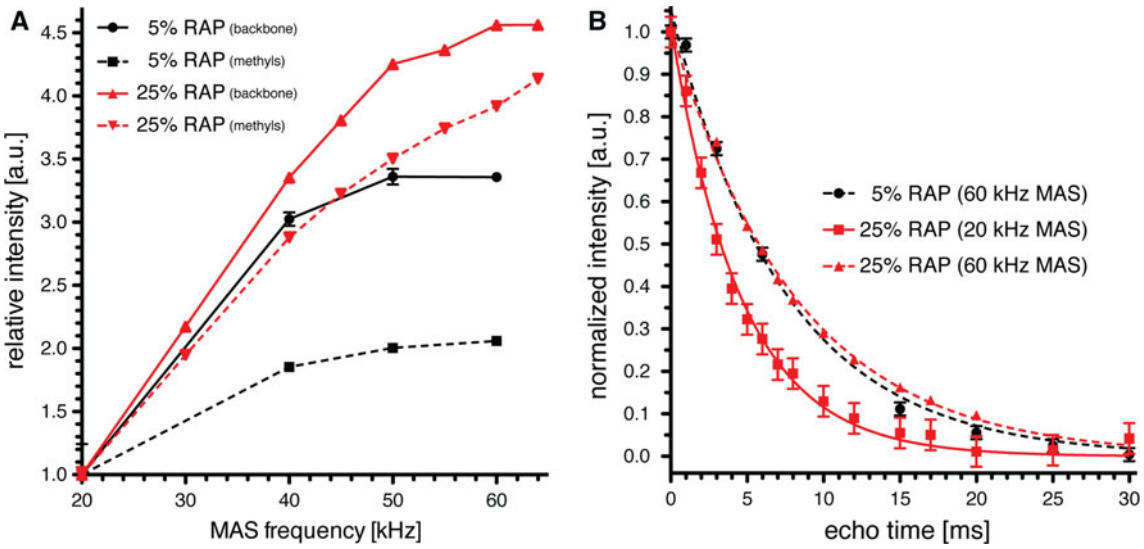

Fig. 1 Bulk sensitivity and ^{1}H T_2 times as a function of the MAS frequency for SH3 RAP samples grown on M9 medium containing either 5 or 25 % H_2O, respectively. **a** Integral intensity for backbone and methyl resonances for the first FID from a ^{1}H,^{13}C HMQC experiment as a function of the MAS frequency. The signal intensity reaches a plateau at a MAS frequency of ~40 (~50) kHz for the 5 % (25 %) RAP sample. The sensitivity gain amounts to a factor of ~3.5 (~4.5) and ~2.0 (~4.0) for backbone and methyl resonances. **b** ^{1}H signal dephasing in a T_2 echo experiment at 20 and 60 kHz. The T_2 time for the 25 % RAP sample increases from 4.6 to 8.2 ms at higher spinning frequencies and becomes comparable to the bulk T_2 of the 5 % RAP sample (7.5 ms)

non-exchangeable sites and partial deuteration of exchangeable sites allow to reduce the proton linewidths to 20–40 Hz in microcrystalline proteins (Chevelkov et al. 2006; Schanda et al. 2009; Akbey et al. 2010; Knight et al. 2011; Lewandowski et al. 2011). This approach is not only applicable to microcrystalline protein samples, but can also successfully be implemented for investigations of membrane proteins and amyloid fibrils (Linser et al. 2011b). Aliphatic protons are most often of interest for studies of protein structure (Asami et al. 2010; Huber et al. 2011; Linser et al. 2011a), dynamics or interactions. Partial deuteration of non-exchangeable sites (Agarwal et al. 2008b; Asami et al. 2010) yields ^{1}H linewidths of 25–60 Hz at moderate MAS (magic angle spinning) frequencies of 20–24 kHz, which is the upper limit for a 3.2 mm rotor. At these frequencies, the heteronuclear ^{1}H, ^{13}C and ^{1}H, ^{15}N dipolar coupling Hamiltonians are averaged.

Unlike heteronuclear dipolar couplings, which are suppressed already at moderate MAS frequencies, decoupling of homonuclear ^{1}H,^{1}H dipolar couplings would require MAS frequencies of >100 kHz and high external fields (>20 T). Nowadays 1.3 mm rotors are commercially available, offering a maximum rotation frequency of about 60 kHz.

We introduced recently the RAP (Reduced Adjoining Protonation) labeling scheme (Asami et al. 2010), which yields randomly protonated protein samples in a deuterated matrix. Here, we investigate the signal-to-noise and linewidth dependence of microcrystalline samples of the chicken α-spectrin SH3 domain for different concentrations of H_2O in the bacterial growth medium and MAS frequencies up to 60 kHz. We find a global optimum in sensitivity and resolution for RAP samples grown on 15–25 % H_2O in the M9 medium, and achieve an experimental ^{1}H linewidth on the order of 40–50 Hz.

1.3 mm rotors (1.6 μL) have a ~20 times smaller active volume, in comparison to 3.2 mm rotors (30 μL). Experimentally, however, only a 4–5 times higher sensitivity is observed for a sample in a 3.2 mm probe in ^{1}H detected experiments at 20 kHz MAS, compared to a sample in a 1.3 mm probe at the same rotation frequency. Increase of the MAS frequency from 20 to 60 kHz yields an increase in sensitivity by a factor of ~4–4.5 in INEPT-based sequences, yielding very similar absolute intensities for a sample in a 1.3 and a 3.2 mm rotor. In addition to reduced ^{1}H dipolar dephasing at high MAS frequencies, this enhancement is also attributed to a higher efficiency of the 1.3 mm probe (Hoult and Richards 1976).

Materials and methods

Sample preparation

Randomly protonated chicken α-spectrin was produced, as described earlier (Chevelkov et al. 2006; Asami et al. 2010). In brief, protein expression was carried out with 5/95 %, 15/85 %, 25/75 % H_2O/D_2O in M9 medium to produce the 5, 15, 25 % RAP sample, respectively. Prior to crystallization in 100 % D_2O, all samples were lyophilized two times in D_2O at pH 3.5. The final microcrystals were

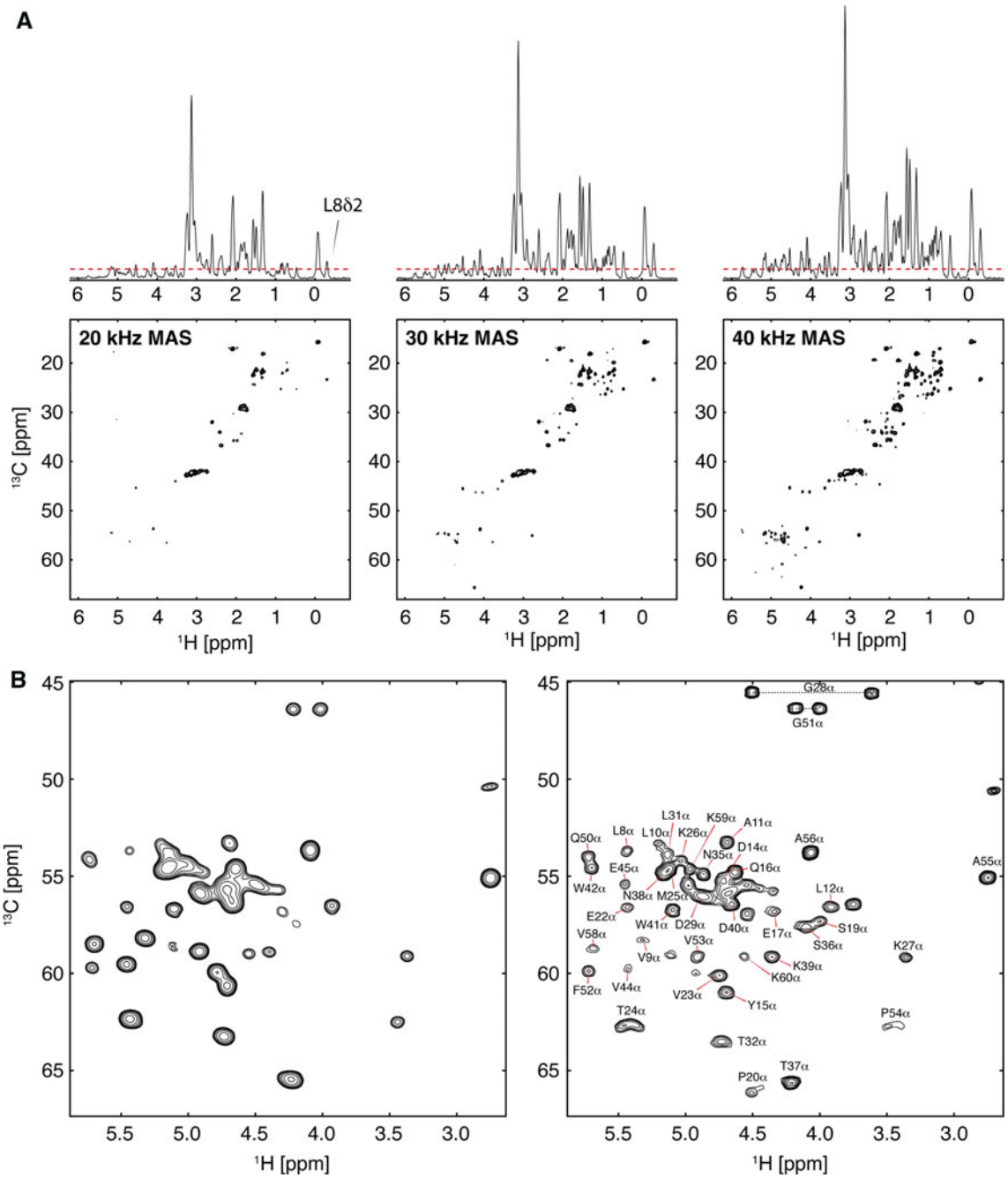

Fig. 2 Sensitivity and resolution for SH3 RAP samples as a function of the MAS frequency and for different external magnetic field strengths. **a** 2D ^{1}H,^{13}C HMQC spectra for a 25 % RAP sample at different MAS rotation frequencies. The *top row* shows the projection onto the ω_2 dimension for the respective 2D spectrum. The *dashed red line* depicts the first contour level, which was set to be equal for all spectra. We observe a significant increase in sensitivity for both backbone and sidechain resonances. **b** ^{1}Hα,^{13}Cα backbone region of a 5 % RAP sample at 20 kHz MAS and a ^{1}H Larmor frequency of 600 MHz (*left*), compared to a spectrum of a 25 % RAP sample at 40 kHz and 850 MHz (*right*), respectively. We observe an improved resolution at higher spinning frequencies and magnetic fields, even though a less diluted sample was employed. The assignments were obtained from a 3D HCC experiment (Asami and Reif 2012)

packed into three 1.3 mm rotors by ultracentrifugation for ~20 min at a relative centrifugal force of ~135,000*g*, employing an ultracentrifuge device (Bockmann et al. 2009).

To investigate the tightness of seal of 1.3 mm rotors at high MAS frequencies, two different glues were utilized, which are referred to as glue "A" and "B". Glue "A" is a fast gluing ("UHU plus schnellfest 2-K-Epoxidharzkleber",

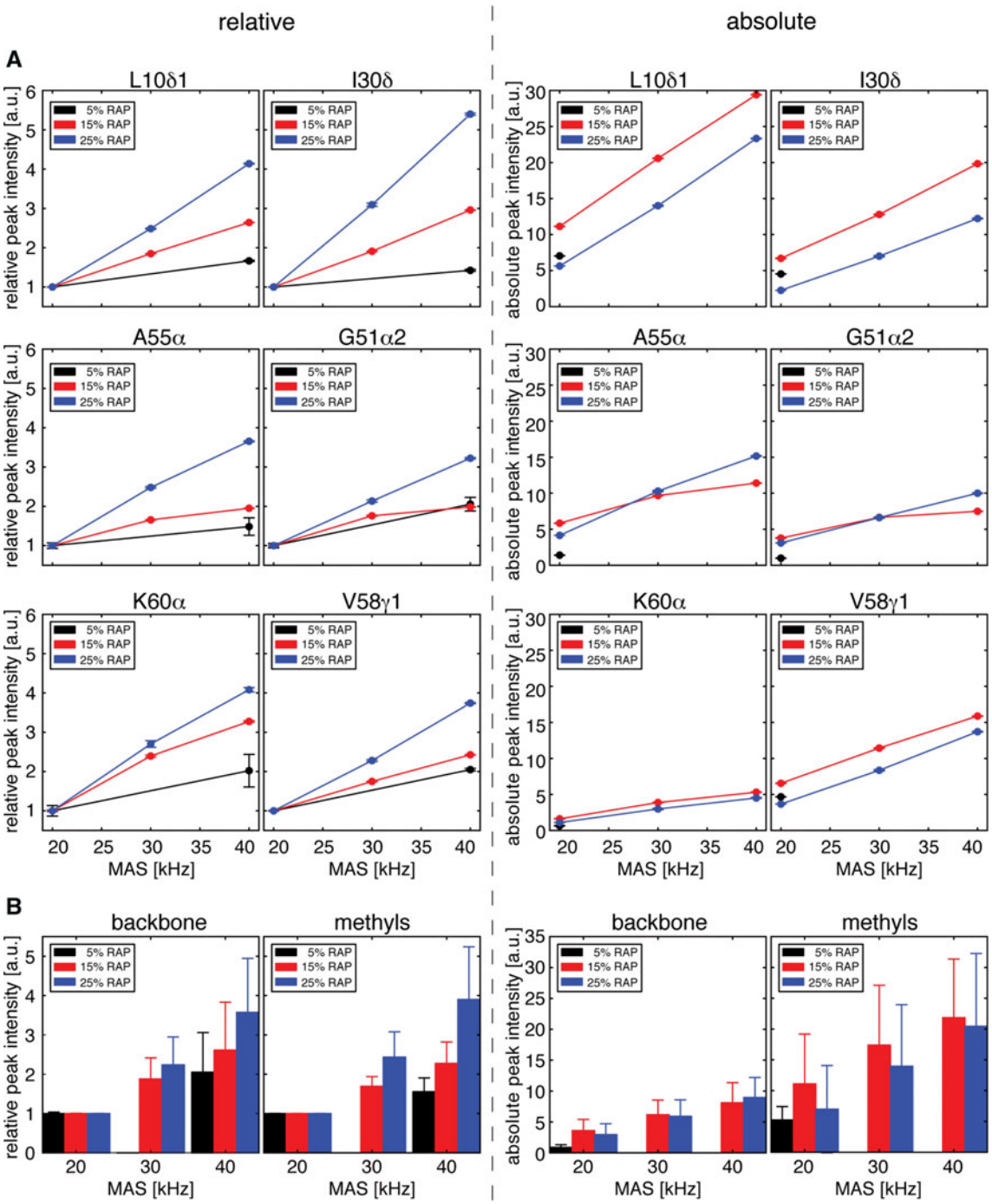

Fig. 3 **a** MAS dependent signal intensities for individual peaks in 5, 15 and 25 % SH3 RAP samples, extracted from a 2D $^{1}H,^{13}C$ HMQC experiment. In the *left column*, the signal intensities are normalized with respect to their intensities at 20 kHz MAS. The *right column* shows absolute signal intensities in arbitrary units. **b** Average peak intensities for backbone and methyl groups for different RAP samples at a relative (*left*) and an absolute scale (*right*), according to the values in Table 1. Absolute intensities are normalized using direct excitation ^{13}C 1D experiments

UHU®) and glue "B" a slowly gluing epoxy ("slow-setting epoxy adhesive", Araldite®), the latter requires at least 12 h to set, unlike glue "A", which requires a few minutes. Three different 1.3 mm rotors were filled with water. Two rotors were glued either with glue "A" or "B". One rotor was kept untreated as a control. Rotor "B" was measured for >12 h after gluing. For the protein samples, only glue "B" was employed. For comparison,

Table 1 Average gain in sensitivity for a 5, 15 and 25 % RAP sample, respectively, at increasing MAS frequencies

		Relative			Absolute		
		20 kHz	30 kHz	40 kHz	20 kHz [a.u.]	30 kHz [a.u.]	40 kHz [a.u.]
Backbone	5 % RAP	1.0 ± 0.0	–	2.1 ± 1.0	0.9 ± 0.4	–	–
	15 % RAP	1.0 ± 0.0	1.9 ± 0.5	2.6 ± 1.2	3.6 ± 1.8	6.2 ± 2.4	8.1 ± 3.2
	25 % RAP	1.0 ± 0.0	2.2 ± 0.7	3.6 ± 1.4	3.0 ± 1.8	5.9 ± 2.7	9.0 ± 3.2
Methyls	5 % RAP	1.0 ± 0.0	–	1.6 ± 0.3	5.2 ± 2.2	–	–
	15 % RAP	1.0 ± 0.0	1.7 ± 0.2	2.3 ± 0.5	11.1 ± 8.1	17.4 ± 9.7	21.9 ± 9.5
	25 % RAP	1.0 ± 0.0	2.4 ± 0.6	3.9 ± 1.3	7.0 ± 7.1	14.0 ± 10.0	20.5 ± 11.8

The absolute average X is determined as $\frac{1}{N}\sum_{i=1}^{N} x_{i,j}$, the relative as $\frac{1}{N}\sum_{i=1}^{N} x_{i,j}/x_{i,1}$, where N refers to the number of resonances, $x_{i,j}$ to the absolute signal intensity for residue i. $j = 1, 2, 3$ refers to the MAS frequencies 20, 30, 40 kHz. The error in the determination of the signal intensities was estimated as $\frac{1}{\sqrt{N}}\Delta n + \frac{1}{N}\sqrt{\sum_{i=1}^{N}(x_i - X)^2}$, where Δn refers to the noise level, x_i to the individual peak intensity and X to the average intensity. The absolute intensities were scaled according to intensities in directly excited ^{13}C 1D spectra. A graphic representation of these values is given in Fig. 3b

glue "A" was used once for a protein sample, as shown in Fig. 11b.

NMR spectroscopy

NMR experiments were carried out using Bruker Biospin Avance spectrometers operating at ^{1}H Larmor frequencies of 500 and 850 MHz, respectively, using a commercial 1.3 mm triple-resonance probe. The 1.3 mm probe of the 850 MHz spectrometer was equipped with an additional external ^{2}H coil (Huber et al. 2012).

At all MAS frequencies, the effective sample temperature was adjusted to ~20 °C, using the chemical shift difference between the solvent resonance and L8δ2. ^{1}H,^{13}C HMQC experiments were performed as described earlier (Asami et al. 2010). The employed rf fields on the ^{1}H and ^{13}C channels for hard pulses were ~80–90 and ~80–100 kHz, respectively. Low-power ^{1}H, ^{2}H and ^{13}C decoupling of 1–3 kHz was applied, using the WALTZ-16 decoupling scheme (Shaka et al. 1983).

For normalization of the absolute signal intensities of the different samples, ^{13}C 1D spectra were recorded for the 5, 15 and 25 % RAP sample, without ^{1}H and ^{2}H decoupling. For these experiments, a recycle delay of 30 s was employed, setting the MAS frequency to 40 kHz.

Data analysis

The spectra were processed with NMRPipe (Delaglio et al. 1995) and analyzed by CCPNMR v2.1.5 (Vranken et al. 2005) and in-house Python scripts, using the I/O routines of nmrglue v0.2 (Helmus and Jaroniec 2011). To compensate for the magnet drift, we corrected the relative frequency shift for each increment of the 2D ^{1}H, ^{13}C HMQC by adding a frequency offset, that is calculated using a fifth order polynomial function. The parameters for the offset correction were determined using the resolved L8δ2 methyl resonance.

Numerical simulations

Numerical simulations were carried out using SIMPSON (Bak et al. 2000). The employed four-nucleus spin system was created with SIMMOL (Bak et al. 2002), using the proton coordinates of lysine, where only the ^{1}Hα, ^{1}Hβ1, ^{1}Hβ2 and ^{1}Hγ1 nuclei were retained, setting their isotropic chemical shift values to 5, 3.5, 3.4 and 2.5 ppm, respectively. Only the dipolar couplings for ^{1}Hα–^{1}Hβ1, ^{1}Hα–^{1}Hβ2, ^{1}Hα–^{1}Hγ1, ^{1}Hβ1–^{1}Hγ1, ^{1}Hβ2–^{1}Hγ1 were considered and set according to the distance of the respective pair of nuclei (Fig. 7). The ^{1}Hα linewidth was simulated as a function of the MAS (20–70 kHz) and ^{1}H Larmor frequency (400–1,000 MHz). Furthermore, the simulation was performed with an altered spin system, in which ^{1}Hβ2 was substituted by a deuteron. The ^{1}H,^{2}H dipolar couplings were adjusted accordingly and a quadrupolar coupling constant of 150 kHz was assumed.

Results and discussion

To investigate the achievable sensitivity and resolution of randomly protonated RAP samples, α-spectrin SH3 was grown using different amounts of H_2O in the M9 minimal medium (5, 15, 25 %). 1D ^{1}H,^{13}C HMQC spectra were recorded between 20 and 64 kHz MAS rotation frequencies. Figure 1a shows the bulk sensitivity for backbone and methyl resonances under these conditions. The spectra reveal, that higher MAS frequencies are beneficial for sensitivity. For the 5 and 25 % RAP sample, the signal increases up to a plateau at a MAS frequency of ~40 and ~50 kHz, respectively. The sensitivity gain is ~3.5

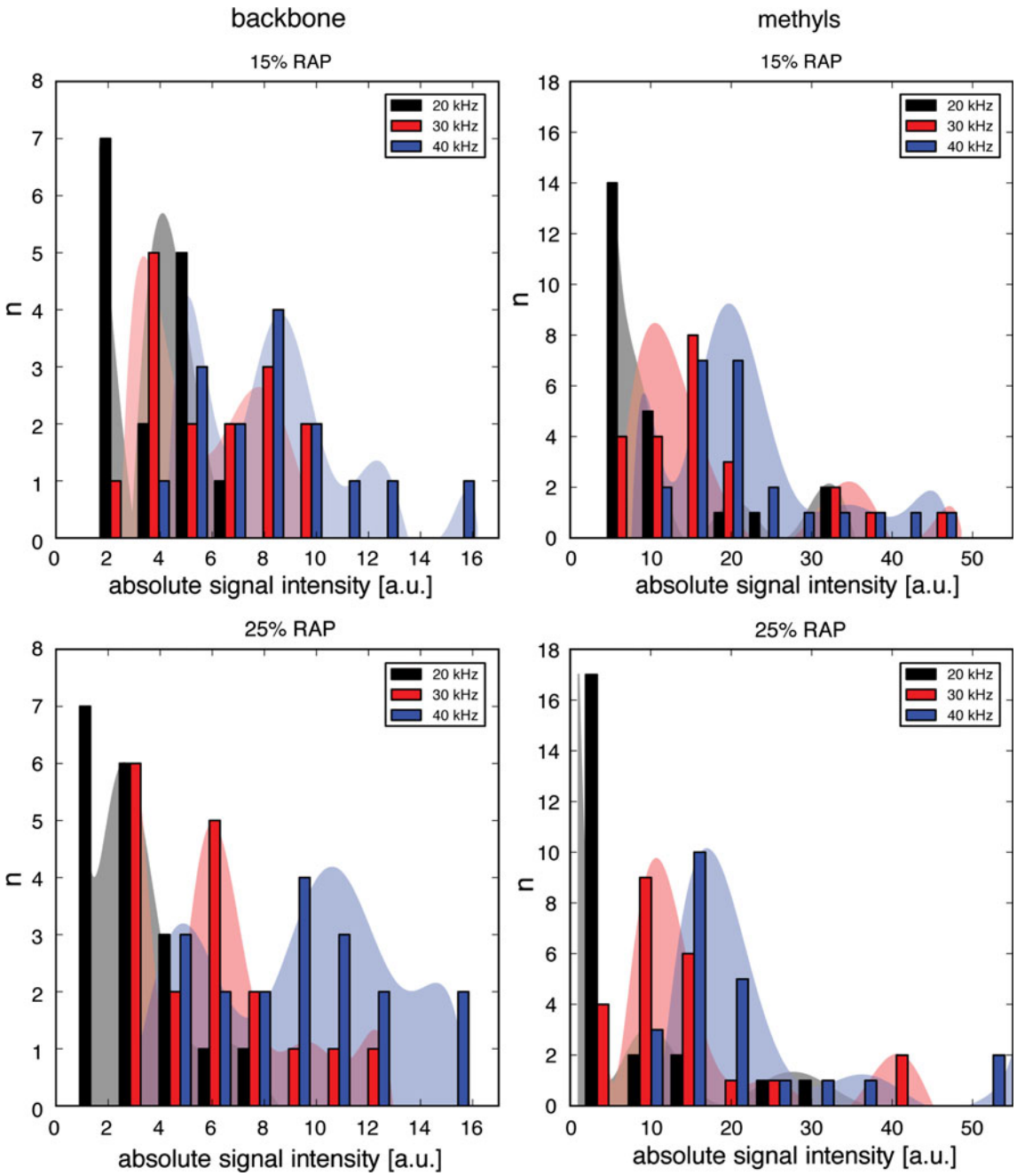

Fig. 4 Distribution of absolute signal intensities in 15 and 25 % RAP samples at different MAS frequencies, with backbone and methyl resonances separated in the *left* and *right* column, respectively. The number of bins is set to ten for all plots

(∼4.5) and ∼2.0 (∼4.0) fold for backbone and methyl resonances for the 5 % (25 %) RAP sample. This progression is expected, since the ^{1}H,^{1}H dipolar network in the 5 % RAP sample is extensively diluted. Therefore rotational averaging of the dipolar Hamiltonian has a smaller impact on dipole mediated linebroadening and hence the signal-to-noise ratio, as compared to less diluted samples, such as the 25 % RAP sample.

The effective ^{1}H T_2 time for the 5 and the 25 % RAP samples at 20 and 60 kHz rotation frequency was determined using a spin echo experiment (Fig. 1b). For this purpose, the HMQC scheme was modified by insertion of an echo, prior to the first $1/2J_{HC}$ delay. The T_2 time for the 25 % RAP sample increases from 4.6 to 8.2 ms at 60 kHz and becomes comparable to the bulk T_2 of the 5 % RAP sample (7.5 ms at

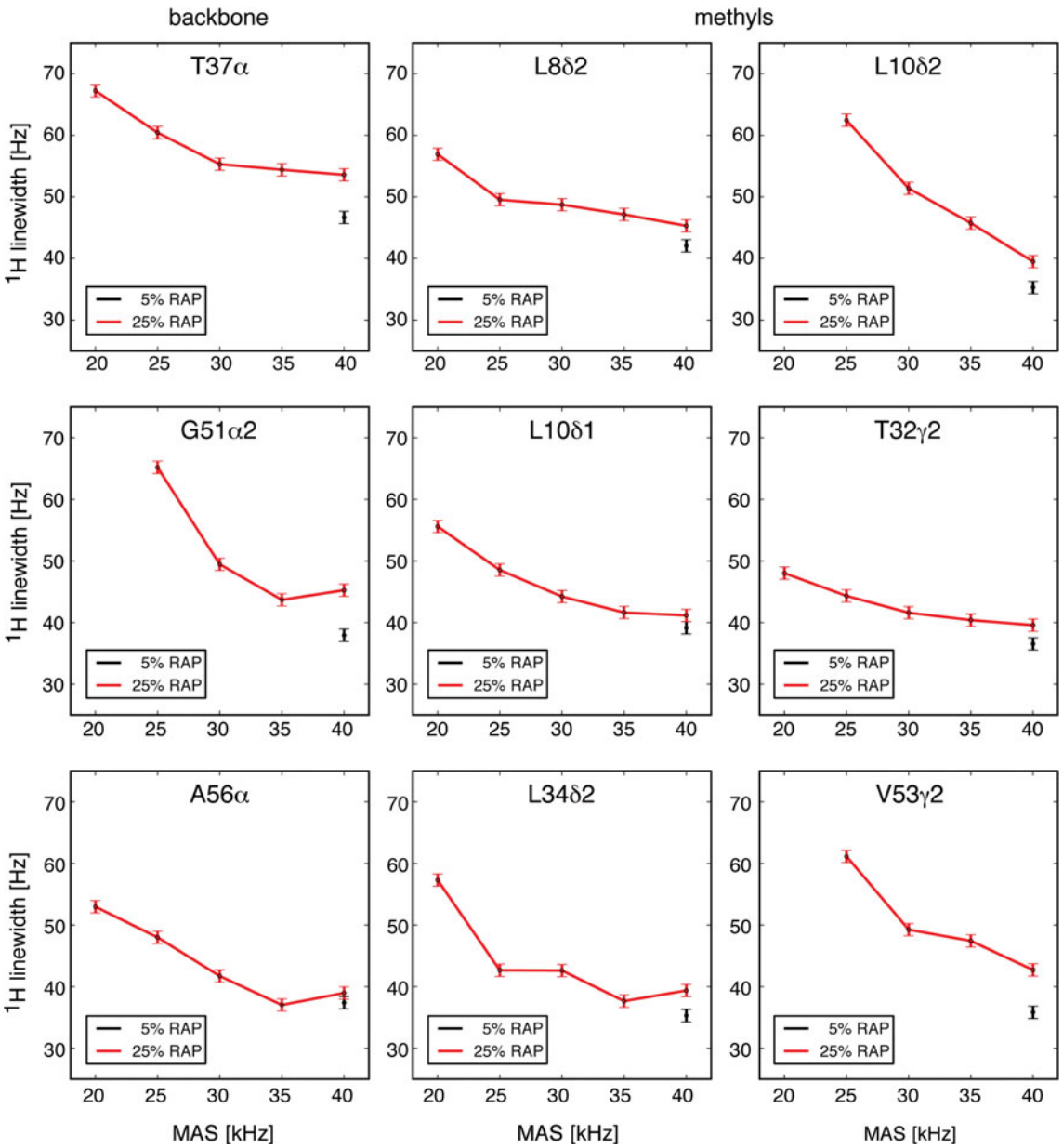

Fig. 5 ^{1}H linewidth as a function of the MAS frequency for a 5 and 25 % RAP sample of α-spectrin SH3

60 kHz). This indicates, that homogeneous linebroadening is already averaged at a MAS frequency of 60 kHz.

As dipolar relaxation through protons is the major source for relaxation for aliphatic sites, ^{1}H T_1 times are expected to increase with higher MAS frequencies, which potentially compromises the sensitivity per unit time in ^{1}H excited experiments. However, for the 25 % RAP sample, the bulk ^{1}H T_1 time increases experimentally only insignificantly from ∼0.8 to ∼0.9 s.

Figure 2a shows 2D ^{1}H,^{13}C HMQC spectra, recorded for a 25 % RAP sample, when increasing the MAS frequency from 20 to 40 kHz. The top row represents the 1D projections of the respective 2D spectra. The first contour level is depicted in the projections by a dashed line (in red), which is kept at an equal absolute signal intensity for all plots. Obviously, the signal-to-noise ratio improves with higher MAS frequencies, in particular for the ^{1}Hα,^{13}Cα backbone region, alongside with a significant improvement of the spectral resolution, as can be seen in Fig. 2b. Here, the backbone region of a 2D ^{1}H, ^{13}C HMQC spectrum of a 5 % RAP sample at 20 kHz MAS and a ^{1}H Larmor frequency of 600 MHz (left) is compared to a spectrum of a 25 % RAP sample at 40 kHz and 850 MHz (right), respectively. The backbone resolution is significantly

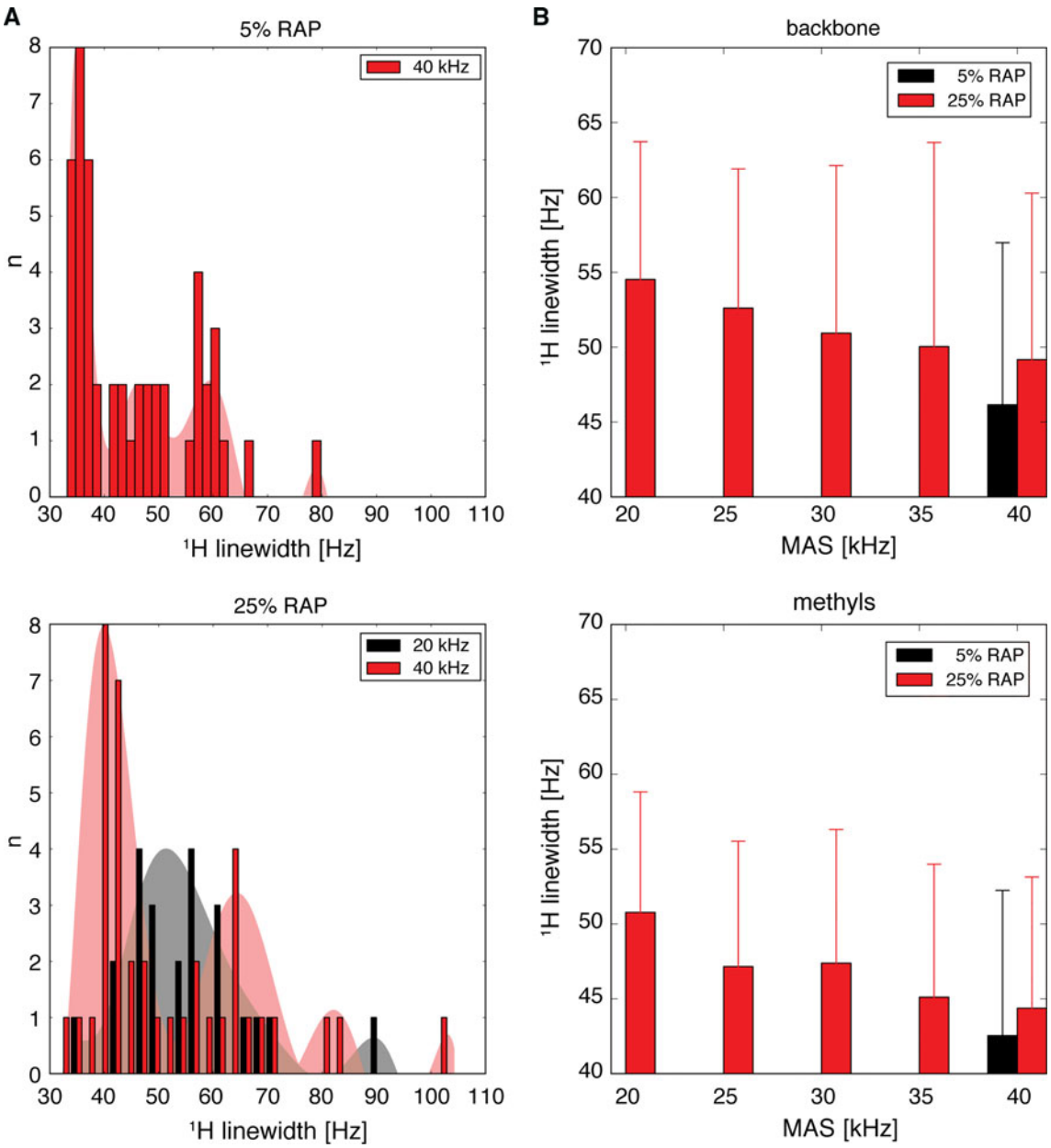

Fig. 6 **a** Distribution of the ^{1}H linewidth for a 5 and 25 % RAP sample of α-spectrin SH3 at 20 and 40 kHz. **b** Average ^{1}H linewidth in the MAS frequency range of 20–40 kHz. Backbone and methyl resonances are plotted separately

improved at 40 kHz, even though a less diluted sample was employed. This is due to an increased effective ^{13}Cα T_2 time and the higher external magnetic field strength.

In Fig. 3a, the MAS dependent signal intensity is represented for individual residues. In the left column, the relative peak intensities are plotted. As expected, the highest relative sensitivity for the backbone as well as for methyl resonances is achieved for the 25 % RAP sample. A less pronounced gain is observed for the 15 and 5 % RAP sample, respectively. On average (Fig. 3b), the relative gain in sensitivity is on the order of 2–4 fold (Table 1). Since methyl groups undergo a fast rotation around their three-fold axis, methyl protons experience a reduced dipolar coupling $d_{\mathrm{met}} = |d_{\mathrm{CH}} \cdot \frac{1}{2}(3\cos^2\theta - 1)| \approx \frac{1}{3}d_{\mathrm{CH}}$ ($\theta = 109.5°$). Therefore, effectively a larger gain is observed for backbone resonances in comparison to methyls.

In order to find the optimum degree of protonation in terms of absolute signal intensities, we plotted the distribution of the absolute signal intensities for the 15 and 25 % RAP sample in Fig. 4. Here, the intensities have been scaled according to the amount of protein in the rotor (see "Materials and methods"). Clearly, a shift to higher

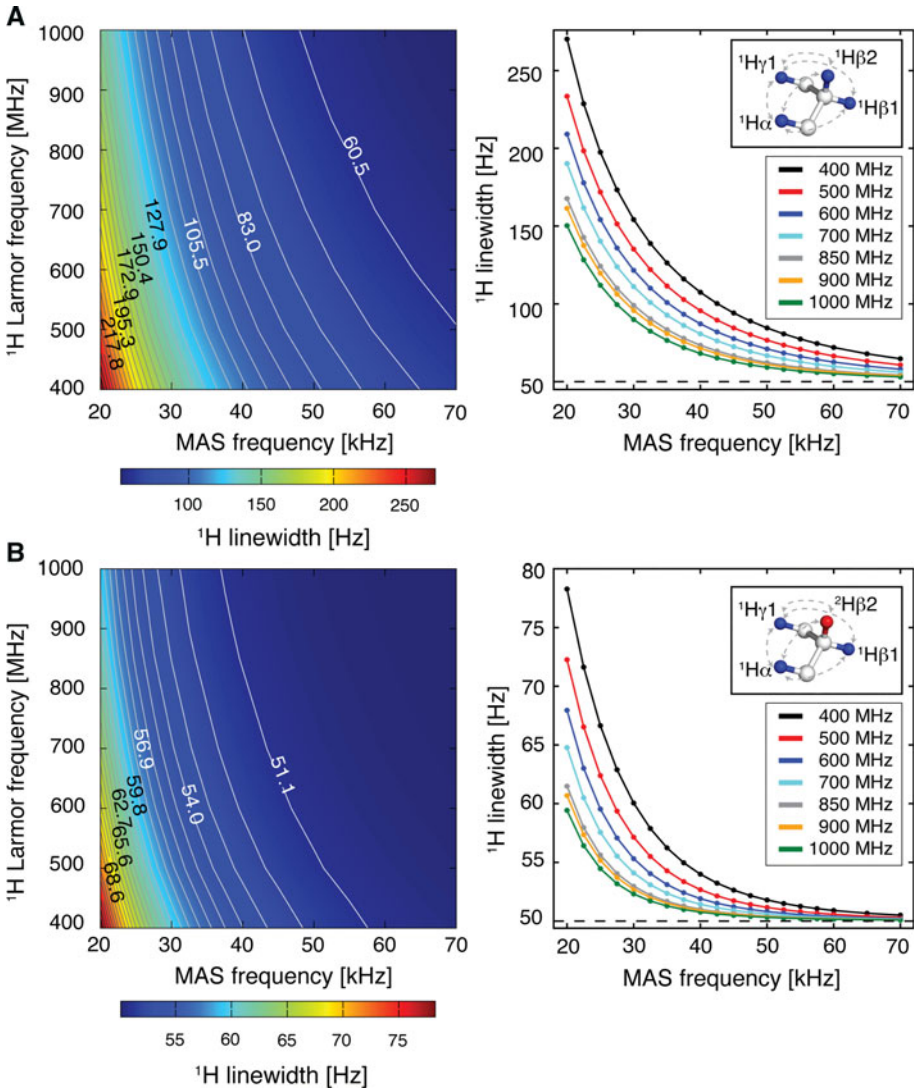

Fig. 7 ^{1}H linewidth as a function of the MAS and the ^{1}H Larmor frequency, simulated for the indicated four spin system. **a** Simulation carried out using four ^{1}H spins. **b** Simulation performed with three ^{1}H spins and one ^{2}H spin. For this simulation, ^{1}Hβ2 was substituted by a deuteron. *Dashed lines* in the structure indicate the dipolar couplings employed in the simulation. For apodization a linebroadening of 50 Hz was applied (*dashed line* in the simulation). In all cases, the ^{1}H linewidth was determined for the ^{1}Hα resonance

intensities is observed for higher MAS frequencies for both samples. Evidently, at 20 kHz MAS the number of high intensity peaks for backbone and methyls is larger for the 15 % in comparison to the 25 % RAP sample. At a MAS frequency of 40 kHz, the average sensitivity of backbone resonances reaches its maximum value for the 25 % RAP sample, and the methyl sensitivity has its optimum for a 15 % RAP sample.

Dipole mediated linebroadening contributes significantly to the detected ^{1}H linewidth, whereas the linewidth approximately scales linearly with the rotor period (Ernst et al. 2001; Reif and Griffin 2003). Along these lines, the ^{1}H linewidth of a 25 % RAP sample was determined as a function of the MAS frequency. As can be seen for backbone as well as for methyl resonances, the linewidth reduces significantly for higher spinning frequencies (Fig. 5). The resolution seems to approach an asymptotic limit above 40 kHz. At 40 kHz, the linewidth of the 25 % RAP sample approaches the average linewidth determined for the 5 % RAP sample (Fig. 6a). The achievable ^{1}H linewidth at 40 kHz MAS for a 25 % RAP sample is on the order of (49 $\pm$ 11) Hz for the backbone, and (44 $\pm$ 9) Hz for methyl protons, respectively (Fig. 6b). Thus, high MAS frequencies almost compensate linebroadening effects of the less dilute sample.

Numerical simulations show similar results for the ^{1}H linewidth at increasing MAS rotation frequencies. The ^{1}H linewidth was determined for a proton within a four-spin system, as a function of MAS and ^{1}H Larmor frequency. The spin system was created with SIMMOL (Bak et al. 2002), using proton coordinates of a lysine molecule, and simulated by SIMPSON (Bak et al. 2000). For the simulations in Fig. 7a the spin system was composed of four proton spins, as depicted by the structural model, whereas for Fig. 7b the ^{1}Hβ2 proton was substituted by a deuteron. As expected, high spinning frequencies, as well as high

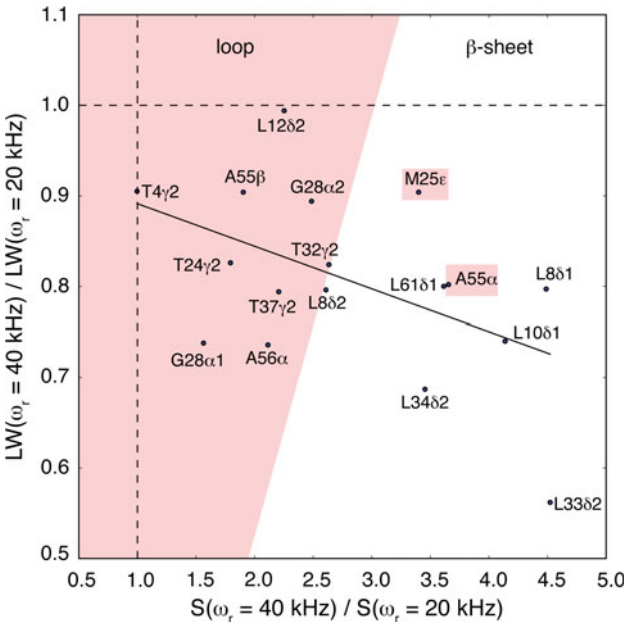

Fig. 8 Relation between the ratio of ^{1}H linewidth and the gain in sensitivity for a 25 % RAP sample, measured at a MAS frequency of 20 and 40 kHz. Overall, the gain in sensitivity and the reduction in linewidth are correlated. The *shaded area* in the diagram highlights residues, which are located in loop regions

magnetic fields, are favorable in terms of resolution, as the dipole mediated linebroadening is almost suppressed for both spin systems. However, replacing a single proton by a deuteron leads to a significant reduction of the ^{1}H linewidth, especially at low spinning frequencies and external magnetic fields.

As expected, sensitivity and resolution are correlated upon change of the MAS rotation frequency (Fig. 8). For accuracy, peaks with high signal-to-noise ratios were selected. The approximate clustering of the population into loop and β-sheet indicates, that fast spinning has a greater influence on resonances of residues, which are located in β-sheets, than for residues in loops. This is presumably due to a higher rigidity of the β-sheets. For example, L33δ2 and L10δ1, which reside in a β-sheet, are strongly MAS-dependent, unlike L12δ2, which is found in a loop region.

In extensively deuterated microcrystalline protein samples, the carbon linewidth is essentially determined by homonuclear scalar couplings to adjacent carbon nuclei, since at high MAS frequencies and magnetic fields the ^{13}C,^{13}C dipolar couplings do not contribute significantly to the ^{13}C linewidth. Selectively labeled precursors, such as [2]-^{13}C or [1,3]-^{13}C glycerol (LeMaster and Kushlan 1996; Hong and Jakes 1999; Castellani et al. 2002), could be employed to isotopically label primarily non-consecutive carbon nuclei in the protein and to remove ^{13}C, ^{13}C scalar couplings. For consecutively carbon labeled samples various homonuclear *J*-decoupling techniques have been suggested for solid-state samples (Straus et al. 1996; Chevelkov et al. 2005; Igumenova and McDermott 2005; Shi et al. 2008; Laage et al. 2009; Kehlet et al. 2011; Asami and Reif 2012). For backbone ^{13}Cα carbons, evolution of the ^{13}CO and ^{13}Cβ coupling can be suppressed by application of bandselective pulses (Asami and Reif 2012). Sidechain carbons are more difficult to decouple due to the chemical shift overlap of the *J*-coupled atoms. In principle, constant-time experiments allow to suppress the evolution of *J*-couplings (Vuister and Bax 1992), but require long ^{13}C coherence lifetimes and high-power decoupling on the order of 100–150 kHz during the constant-time periods (Tian et al. 2009), even for deuterated proteins (Tang et al. 2010). To estimate the ^{13}C coherence lifetimes, we performed 1D constant-time HSQC experiments (Vuister and Bax 1992) for a 5 and 25 % RAP sample at 20 and 60 kHz MAS (Fig. 9), respectively. The constant-time delay was set to 28.6 ms, according to $1/J_{C\alpha C\beta}$. At 20 kHz MAS, the resolved signal of L8δ2 is barely detectable in both samples. Overall, all sidechain resonances, especially the methyl resonances in the 25 % RAP sample, exhibit very low peak intensities. Setting the MAS frequency to 60 kHz yields a significant increase of the effective T_2 time for sidechain carbons. The peak intensity of the resolved L8δ2 signal increases up to a factor of $\sim$2 and $\sim$8 for the 5 and 25 % RAP sample, respectively.

In addition to linewidth and sensitivity, the isotopomeric purity, and thus, the spectral quality, has to be taken into account to identify the ideal amount of H_2O in the bacterial growth medium. For this labeling scheme, a distribution of the isotopomers $^{13}CH_3$, $^{13}CDH_2$, $^{13}CD_2H$ and $^{13}CD_3$ is obtained. However, in the employed experiments, only isotopomers, that contain protons, are detected. The proton concentration in RAP samples can be adjusted by the $[H_2O]/[D_2O]$ ratio in the M9 medium (Asami et al. 2010). Neglecting the residual 3 % protonation originating from the 97 % deuterated [^{13}C]-glucose (Agarwal and Reif 2008a), the isotopomeric ratio of $^{13}CD_2H$ to $^{13}CDH_2$ can be determined to first order approximation, by calculating $3(1\text{-}p)^2p/3(1\text{-}p)p^2$, where p corresponds to $[H_2O]/[D_2O]$. As can be seen in Fig. 10a, $^{13}CD_2H$ is the highest populated isotopomer for the employed 5–25 % RAP samples. This also is found experimentally (Asami et al. 2010).

For a 25 % RAP sample, the averaged peak volume ratio $[^{13}CD_2H]/[^{13}CDH_2]$ is on the order of three. The $^{13}CDH_2$ isotopomer is sufficiently populated for detection. In a 2D ^{1}H,^{13}C HMQC spectrum recorded at a spinning frequency of 40 kHz this lower populated isotopomer becomes visible (Fig. 10b). To determine the ratio of isotopomers, the experimentally determined peak ratio was multiplied by a factor of two to account for the number of bound protons.

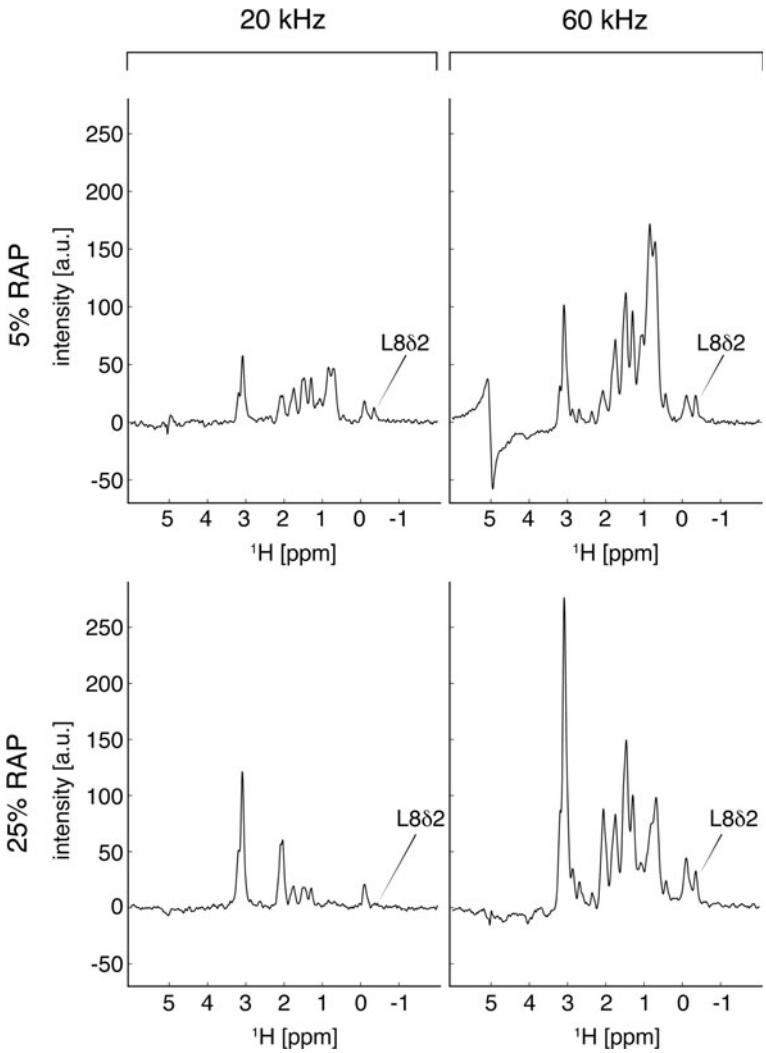

Fig. 9 First increment of a constant-time $^{1}H,^{13}C$ HSQC experiment of a 5 and 25 % RAP sample of a microcrystalline sample of the α-spectrin SH3 domain at 20 and 60 kHz MAS frequency. The constant-time period $T = 1/J_{CC}$ was set to 28.6 ms. The gain in sensitivity for L8δ2 is on the order of $\sim$2 and $\sim$8 fold for the 5 and 25 % RAP sample, respectively

High MAS frequencies imply strong centrifugal forces on the rotor and the contained sample. The g-force that a sample in a 1.3 mm rotor at 60 kHz experiences is about four times larger than the force for a sample in a 3.2 mm rotor at 20 kHz (calculated for the inner radii). It can therefore be assumed, that the tightness of seal deteriorates with faster spinning. Since the solvent matrix is essential for protein stability, solvent leakage can be problematic for protein samples. Therefore the influence of two different epoxy glues on impermeability was investigated (Fig. 11a). Three 1.3 mm rotors were filled with water and either glued with glue "A" (UHU epoxy), glue "B" (Araldite) or kept untreated. The left *y*-axis in Fig. 11a depicts the normalized water integral and the right y-axis the MAS frequency.

The untreated rotor shows already after $\sim$5 min a >99.9 % water loss. By contrast, glue "A" provides a significant improvement for the tightness of seal at 20 kHz. However, after $\sim$1 h spinning the remaining water content decreased to about 10 %. Increase of the MAS frequency to 30 kHz induces an almost total loss of the water signal. Glue "B" shows the best performance concerning the tightness of seal. After $\sim$1 h at 60 kHz MAS, the water content remains at $\sim$90 %. After an additional period of $\sim$15 h, the water signal decreases steadily to $\sim$20 %. Rotation induces a lateral force on the solvent, which promotes leakage. This is in particular a problem for samples of pure water without protein. By contrast, the protein will rather be compacted at the wall of the rotor. Subsequently, two 1.3 mm rotors were filled with a 25 % RAP SH3 sample. The rotors were either sealed with glue "A" or "B", respectively. The first increment of a $^{1}H,^{13}C$ HMQC experiment reveals, that the protein in rotor "B" remains stable after several hours spinning at 60 kHz MAS, whereas the protein in rotor "A" becomes denatured after $\sim$1 h (Fig. 11b).

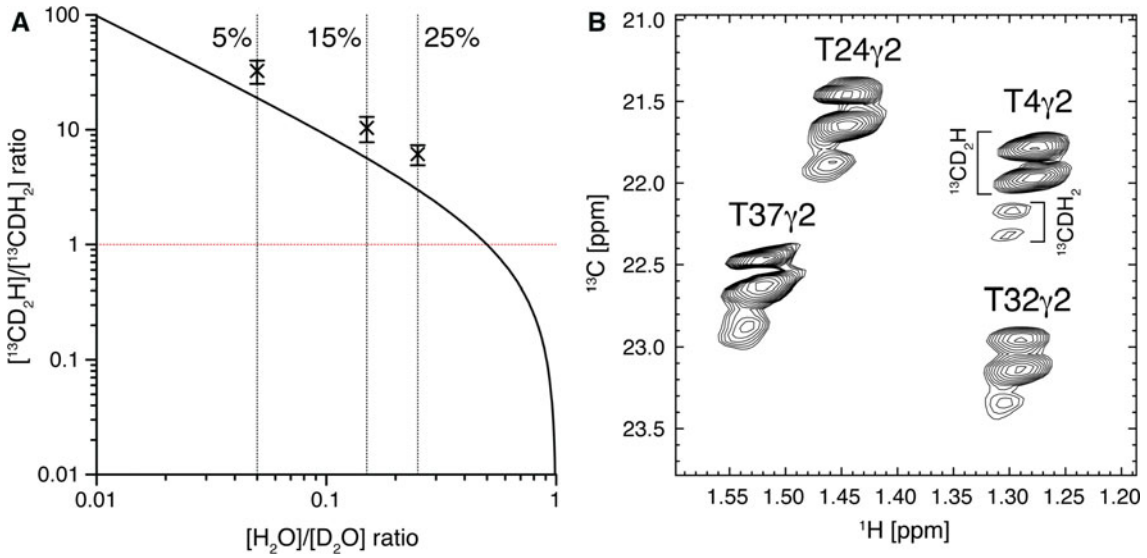

Fig. 10 Isotopomeric mixtures in RAP samples. **a** The ratio of the isotopomers $[^{13}CD_2H]/[^{13}CDH_2]$ is plotted as a function of $[H_2O]/[D_2O]$ in the bacterial growth medium. For a statistic incorporation of protons, this ratio corresponds to $(1\text{-}p)/p$, where p corresponds to $[H_2O]/[D_2O]$. The 5, 15 and 25 % RAP samples are indicated by *dashed vertical lines*. *Error bars* indicate averaged ratios from solution-state and solid-state NMR data, as obtained earlier (Asami et al. 2010). Here, the experimentally determined ratio $[^{13}CD_2H]/[^{13}CDH_2]$ was scaled to account for the number of bound protons (see main text). **b** 2D ^1H,^{13}C HMQC spectrum of a 25 % SH3 RAP sample at 850 MHz ^1H Larmor frequency and 40 kHz MAS. The most populated isotopomers, $^{13}CD_2H$ and $^{13}CDH_2$, can be detected. The isotopomers show the typical isotope induced chemical shift differences of 0.025 and 0.36 ppm (Gardner et al. 1997) in the ^{13}C and ^1H dimension, respectively

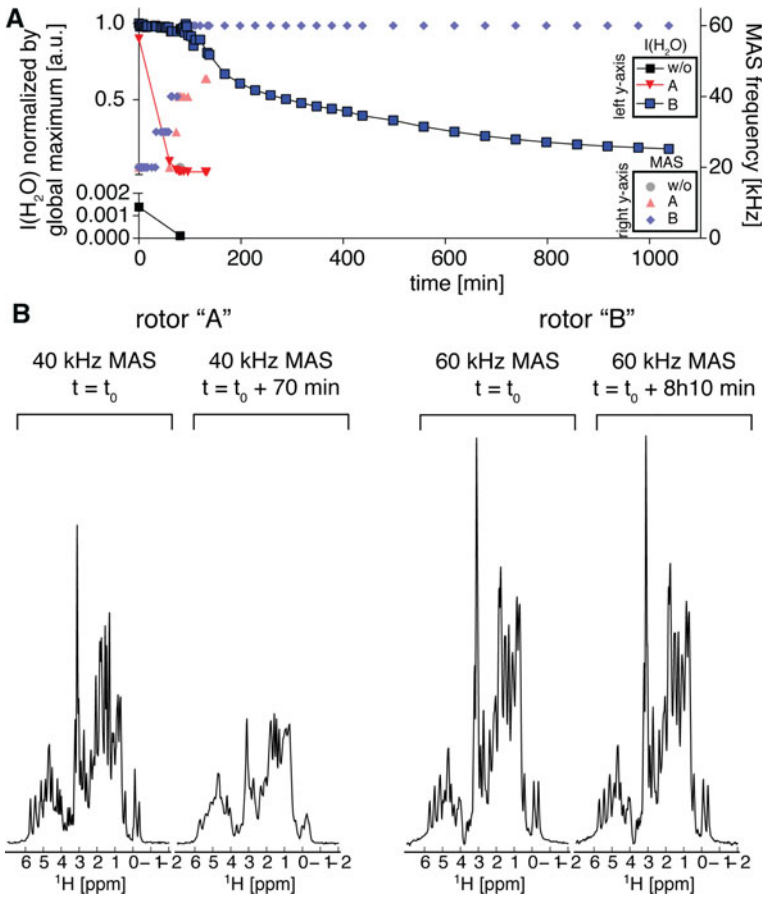

Fig. 11 Tightness of seal of a 1.3 mm rotor at 20–60 kHz MAS employing different procedures for sealing. In the experiments, the *top* and *bottom caps* were either sealed with glue "A" (UHU epoxy), glue "B" (Araldite), or kept unsealed. **a** Water integral of fully water-filled 1.3 mm rotors as a function of time and MAS frequency. Glue "B" induces a significantly higher H_2O tightness. **b** 1D ^1H,^{13}C HMQC spectra of two 25 % RAP SH3 samples sealed with glue "A" (*left*) and "B" (*right*), respectively. Clearly, the sample in rotor "B" remains stable, even after hours at 60 kHz MAS, while the sample in rotor "A" becomes denaturated after minutes and only 40 kHz MAS

Conclusion

We presented a systematic analysis of sensitivity and resolution of different randomly protonated microcrystalline protein samples as a function of the MAS frequency. Not surprisingly, fast MAS spinning is most beneficial for sensitivity and resolution in ^{1}H detected INEPT based ^{1}H,^{13}C correlation experiments, due to the improvement of the effective T_2 times for ^{1}H and ^{13}C, respectively.

We find, that a α-spectrin SH3 RAP sample expressed from a M9 minimal medium with a H_2O content of 15–25 % rotated at 60 kHz MAS yields the best compromise in terms of spectroscopic performance. For the 25 % RAP sample, the relative sensitivity gain at 60 kHz MAS is on average ∼4.5 and ∼4 fold for backbone and methyl resonances, respectively. The ratio of absolute peak intensities for a fully-packed 3.2 mm rotor at 20 kHz MAS (700 MHz) to a 1.3 mm rotor at 60 kHz (850 MHz) amounts to ∼1.1–1.3, whereas the ratio of the active sample volumes is on the order of ∼20. The 3.2 mm rotor was packed by a benchtop centrifuge (∼40,000*g*), while the 1.3 mm rotor was packed by ultracentrifugation (∼135,000*g*). This might account for a factor of 1–2 in the amount of material in the 1.3 mm rotor.

We performed 2D experiments at a MAS rotation frequency of 40 kHz, and determined residue-specific ^{1}H linewidths for a 5 % and a 25 % RAP sample. For the 25 % RAP sample, the average ^{1}H linewidth amounts to 44-49 Hz. The linewidth for the 5 % RAP sample is on the same order, which is supported by the ^{1}H T_2 echo experiments, carried out at 60 kHz MAS.

The highest sensitivity is obtained for the 25 % RAP sample rotated at 60 kHz. Under these conditions, dipole mediated linebroadening is not yet outperforming sensitivity and resolution. Use of a higher relative concentration of H_2O in the bacterial growth medium seems unfavorable, however, due to an increase of the $^{13}CDH_2$ isotopomer, which results in additional resonances and thus in a decrease of resolution.

Due to sample stability and hardware issues, only 1D experiments could be carried out so far at 60 kHz. We expect that, enhanced coherence lifetimes will facilitate solution-state like multi-bond experiments in the future, and allow scalar transfers even for weakly coupled spin systems (Linser et al. 2008; Schanda et al. 2009).

Acknowledgments This research was supported by the Leibniz- and the Helmholtz-Gemeinschaft, the DFG (Re1435, SFB449, SFB740) and the Bio-NMR project (European Commission's Framework Program 7, project number: 261863). We are grateful to the Center for Integrated Protein Science Munich (CIPS-M) for financial support and to Bruker BioSpin for providing measurement time, especially to S. Wegner and G. Althoff for technical support. P.S. acknowledges funding from the French Research Agency (Contract ANR-10-PDOC-011-01 ProtDynByNMR).

References

Agarwal V, Reif B (2008) Residual methyl protonation in perdeuterated proteins for multi-dimensional correlation experiments in MAS solid-state NMR spectroscopy. J Magn Reson 194: 16–24

Agarwal V, Xue Y, Reif B, Skrynnikov NR (2008) Protein side-chain dynamics as observed by solution- and solid-state NMR spectroscopy: a similarity revealed. J Am Chem Soc 130: 16611–16621

Akbey U, Lange S, Franks WT, Linser R, Rehbein K, Diehl A, van Rossum BJ, Reif B, Oschkinat H (2010) Optimum levels of exchangeable protons in perdeuterated proteins for proton detection in MAS solid-state NMR spectroscopy. J Biomol NMR 46:67–73

Asami S, Reif B (2012) Assignment strategies for aliphatic protons in the solid-state in randomly protonated proteins. J Biomol NMR 52:31–39

Asami S, Schmieder P, Reif B (2010) High resolution H-1-detected solid-state NMR spectroscopy of protein aliphatic resonances: access to tertiary structure information. J Am Chem Soc 132:15133–15135

Bak M, Rasmussen JT, Nielsen NC (2000) SIMPSON: a general simulation program for solid-state NMR spectroscopy. J Magn Reson 147:296–330

Bak M, Schultz R, Vosegaard T, Nielsen NC (2002) Specification and visualization of anisotropic interaction tensors in polypeptides and numerical simulations in biological solid-state NMR. J Magn Reson 154:28–45

Bielecki A, Kolbert AC, Levitt MH (1989) Frequency-switched pulse sequences: homonuclear decoupling and dilute spin NMR in solids. Chem Phys Lett 155:341–346

Bockmann A, Gardiennet C, Verel R, Hunkeler A, Loquet A, Pintacuda G, Emsley L, Meier BH, Lesage A (2009) Characterization of different water pools in solid-state NMR protein samples. J Biomol NMR 45:319–327

Bosman L, Madhu PK, Vega S, Vinogradov E (2004) Improvement of homonuclear dipolar decoupling sequences in solid-state nuclear magnetic resonance utilising radiofrequency imperfections. J Magn Reson 169:39–48

Castellani F, van Rossum B, Diehl A, Schubert M, Rehbein K, Oschkinat H (2002) Structure of a protein determined by solid-state magic-angle-spinning NMR spectroscopy. Nature 420: 98–102

Chevelkov V, Chen Z, Bermel W, Reif B (2005) Resolution enhancement in MAS solid-state NMR by application of 13C homonuclear scalar decoupling during acquisition. J Magn Reson 172:56–62

Chevelkov V, Rehbein K, Diehl A, Reif B (2006) Ultrahigh resolution in proton solid-state NMR spectroscopy at high levels of deuteration. Angew Chem Int Ed 45:3878–3881

Delaglio F, Grzesiek S, Vuister GW, Zhu G, Pfeifer J, Bax A (1995) Nmrpipe—a multidimensional spectral processing system based on Unix pipes. J Biomol NMR 6:277–293

Ernst M, Samoson A, Meier BH (2001) Low-power decoupling in fast magic-angle spinning NMR. Chem Phys Lett 348:293–302

Ferguson N, Becker J, Tidow H, Tremmel S, Sharpe TD, Krause G, Flinders J, Petrovich M, Berriman J, Oschkinat H, Fersht AR (2006) General structural motifs of amyloid protofilaments. Proc Natl Acad Sci U S A 103:16248–16253

Franks WT, Wylie BJ, Schmidt HLF, Nieuwkoop AJ, Mayrhofer RM, Shah GJ, Graesser DT, Rienstra CM (2008) Dipole tensor-based atomic-resolution structure determination of a nanocrystalline protein by solid-state NMR. Proc Natl Acad Sci U S A 105:4621–4626

Gardner KH, Rosen MK, Kay LE (1997) Global folds of highly deuterated, methyl-protonated proteins by multidimensional NMR. Biochemistry 36:1389–1401

Helmus JJ, Jaroniec CP (2011) NMR glue, http://code.google.com/p/nmrglue, The Ohio State University

Hong M, Jakes K (1999) Selective and extensive C-13 labeling of a membrane protein for solid-state NMR investigations. J Biomol NMR 14:71–74

Hoult DI, Richards RE (1976) Signal-to-noise ratio of nuclear magnetic-resonance experiment. J Magn Reson 24:71–85

Huber M, Hiller S, Schanda P, Ernst M, Bockmann A, Verel R, Meier BH (2011) A proton-detected 4D solid-state NMR experiment for protein structure determination. ChemPhysChem 12:915–918

Huber M, With O, Schanda P, Verel R, Ernst M, Meier BH (2012) A supplementary coil for (2)H decoupling with commercial HCN MAS probes. J Magn Reson 214:76–80

Igumenova TI, McDermott AE (2005) Homo-nuclear 13C J-decoupling in uniformly 13C-enriched solid proteins. J Magn Reson 175:11–20

Kehlet C, Nielsen JT, Tosner Z, Nielsen NC (2011) Resolution-enhanced solid-state NMR (13)C-(13)C correlation spectroscopy by optimal control dipolar-driven spin-state-selective coherence transfer. J Phys Chem Lett 2:543–547

Knight MJ, Webber AL, Pell AJ, Guerry P, Barbet-Massin E, Bertini I, Felli IC, Gonnelli L, Pierattelli R, Emsley L, Lesage A, Herrmann T, Pintacuda G (2011) Fast resonance assignment and fold determination of human superoxide dismutase by high-resolution proton-detected solid-state MAS NMR spectroscopy. Angew Chem Int Ed Engl 50:11697–11701

Laage S, Lesage A, Emsley L, Bertini I, Felli IC, Pierattelli R, Pintacuda G (2009) Transverse-dephasing optimized homonuclear j-decoupling in solid-state NMR spectroscopy of uniformly 13C-labeled proteins. J Am Chem Soc 131:10816–10817

LeMaster DM, Kushlan DM (1996) Dynamical mapping of E-coli thioredoxin via C-13 NMR relaxation analysis. J Am Chem Soc 118:9255–9264

Levitt MH, Kolbert AC, Bielecki A, Ruben DJ (1993) High-resolution H-1-NMR in solids with frequency-switched multiple-pulse sequences. Solid State Nucl Mag 2:151–163

Lewandowski JR, Dumez JN, Akbey U, Lange S, Emsley L, Oschkinat H (2011) Enhanced resolution and coherence lifetimes in the solid-state NMR spectroscopy of perdeuterated proteins under ultrafast magic-angle spinning. J Phys Chem Lett 2:2205–2211

Linser R, Fink U, Reif B (2008) Proton-detected scalar coupling based assignment strategies in MAS solid-state NMR spectroscopy applied to perdeuterated proteins. J Magn Reson 193:89–93

Linser R, Bardiaux B, Higman V, Fink U, Reif B (2011a) Structure calculation from unambiguous long-range amide and methyl (1)h-(1)h distance restraints for a microcrystalline protein with MAS solid-state NMR spectroscopy. J Am Chem Soc 133:5905–5912

Linser R, Dasari M, Hiller M, Higman V, Fink U, Lopez Del Amo JM, Markovic S, Handel L, Kessler B, Schmieder P, Oesterhelt D, Oschkinat H, Reif B (2011b) Proton-detected solid-state NMR spectroscopy of fibrillar and membrane proteins. Angew Chem Int Ed Engl 50:4508–4512

Reif B, Griffin RG (2003) H-1 detected H-1, N-15 correlation spectroscopy in rotating solids. J Magn Reson 160:78–83

Sakellariou D, Lesage A, Hodgkinson P, Emsley L (2000) Homonuclear dipolar decoupling in solid-state NMR using continuous phase modulation. Chem Phys Lett 319:253–260

Schanda P, Huber M, Verel R, Ernst M, Meier BH (2009) Direct detection of (3 h)J(NC′) hydrogen-bond scalar couplings in proteins by solid-state NMR spectroscopy. Angew Chem Int Ed 48:9322–9325

Shaka AJ, Keeler J, Frenkiel T, Freeman R (1983) An improved sequence for broad-band decoupling: Waltz-16. J Magn Reson 52:335–338

Shi L, Peng X, Ahmed MA, Edwards D, Brown LS, Ladizhansky V (2008) Resolution enhancement by homonuclear J-decoupling: application to three-dimensional solid-state magic angle spinning NMR spectroscopy. J Biomol NMR 41:9–15

Straus SK, Bremi T, Ernst RR (1996) Resolution enhancement by homonuclear J decoupling in solid-state MAS NMR. Chem Phys Lett 262:709–715

Tang M, Comellas G, Mueller LJ, Rienstra CM (2010) High resolution 13C-detected solid-state NMR spectroscopy of a deuterated protein. J Biomol NMR 48:103–111

Tian Y, Chen L, Niks D, Kaiser JM, Lai J, Rienstra CM, Dunn MF, Mueller LJ (2009) J-Based 3D sidechain correlation in solid-state proteins. Phys Chem Chem Phys 11:7078–7086

Vinogradov E, Madhu PK, Vega S (1999) High-resolution proton solid-state NMR spectroscopy by phase-modulated Lee-Goldburg experiment. Chem Phys Lett 314:443–450

Vranken WF, Boucher W, Stevens TJ, Fogh RH, Pajon A, Llinas M, Ulrich EL, Markley JL, Ionides J, Laue ED (2005) The CCPN data model for NMR spectroscopy: development of a software pipeline. Proteins 59:687–696

Vuister GW, Bax A (1992) Resolution enhancement and spectral editing of uniformly C-13-enriched proteins by homonuclear broad-band C-13 decoupling. J Magn Reson 98:428–435

Wasmer C, Lange A, Van Melckebeke H, Siemer AB, Riek R, Meier BH (2008) Amyloid fibrils of the HET-s(218–289) prion form a beta solenoid with a triangular hydrophobic core. Science 319:1523–1526